

WAVE TRANSMISSION OF FIXED BOTTOM-DETACHED BREAKWATERS IN NUMERICAL WAVE FLUME

Zihan Liu, Andrea Esposito, Lorenzo Cappietti

Abstract: This work presents preliminary numerical simulation results on wave interaction with a fixed Bottom-Detached Breakwater (BDB). The purpose of developing fixed BDB is to provide a safe offshore zone for human activities, such as energy production and docking of large vessels, even in extreme weather. The transmission coefficient (k_t) is used to assess the protection performance of the BDB. A two-dimensional Numerical Wave Flume (NWF) was developed by using ANSYS Fluent, validated with existing data and then used for studying the interaction between extreme waves and the BDB. The role of BDB design parameters such as its width and draft, and wave height and wavelength on k_t was investigated. The reliability of the results of k_t was verified by previous experimental study. This study demonstrates the development of a reliable NWF for conducting parametric analysis of BDBs and is a kick-off study for further developing the numerical and experimental study of floating breakwaters.

Keywords: Wave-structure interaction; transmission coefficient; bottom-detached breakwater (BDB); numerical wave flume; computational fluid dynamics

Zihan Liu, University of Florence, Italy, zihan.liu@unifi.it
Andrea Esposito, AM3 Spin-off s.r.l., Italy, andrea.esposito@am3spinoff.com
Lorenzo Cappietti, University of Florence, Italy, lorenzo.cappietti@unifi.it, 0000-0002-3957-5763

Referee List (DOI 10.36253/fup_referee_list)

FUP Best Practice in Scholarly Publishing (DOI 10.36253/fup_best_practice)

Zihan Liu, Andrea Esposito, Lorenzo Cappietti, *Wave transmission of Fixed Bottom-detached Breakwaters in Numerical Wave Flume*, pp. 901-910, © 2024 Author(s), CC BY-NC-SA 4.0, DOI: 10.36253/979-12-215-0556-6.78

1 Introduction

Very Large Floating Structure (VLFS) presents a potential solution for expanding operational space and efficiently use the maritime space, and it could address seawater level rising and land subsidence with a resilient approach [1]. Maritime concrete caissons are the primary components of breakwaters and harbours. The size of existing maritime concrete caissons could reach up to 67 m in length, 35 m in width, and 33 m in height as for the Genova's harbour breakwater (Italy), presently under building (July 2024).

Various studies have proposed methods for predicting the transmission coefficient (k_t) of breakwaters [2-4]. One of the most well-known formulas for predicting k_t , particularly for box-type breakwaters, was derived by Macagno [5-7] using linear wave theory. Ursell [8] developed a formula for predicting the k_t in deep-water regions, identifying relative draft (the ratio of draft to wavelength) as a crucial factor. Carr [6] conducted a foundational study on floating breakwaters in shallow water and derived the first formula for shallow-water conditions. Kolahdooza et al. [6] later improved Carr's formula which offered more accurate predictions of k_t in shallow waters. When compared with laboratory and prototype results, particularly for short waves or large drafts relative to mean sea level, the Macagno's formula predictions were qualitatively correct but generally inaccurate. Ruol et. al [5] proposed a modification factor for Macagno's formula to better predict the k_t of various π -type pontoon floating breakwaters. Ruol's empirical formula accounts for the motion effects of the structure, improving Macagno's formula for application to π -type breakwaters and it has been verified by researchers to predict the k_t of pontoon-type and π -type floating breakwaters [9]. However, it has been observed that in shallow and intermediate waves, Ruol's formula was less accurate than Carr's formula [6]. Paotonan et al. [10] introduced a new type of composite hanging breakwater, which is suspended from transverse and longitudinal beams supported by piles.

To date, most studies have focused on relatively small- and mid-sized breakwater located in intermediate and shallow waters, often within naturally protected marine areas and under mild wave conditions. The interaction between extreme waves and large-sized breakwater should be further explored. In this work, a fixed Bottom-Detached Breakwater (BDB) is considered an ideal precursor to floating breakwaters, with its displacement strictly controlled by mooring and anchor systems. A Computational Fluid Dynamics (CFD) tool, ANSYS Fluent, was used to develop and calibrate a two-dimensional (2D) Numerical Wave Flume (NWF) for generating various waves with high accuracy. The study investigates the influence of wave conditions and BDB dimensions on k_t , including the performance of BDBs with large draft (D_{FB}) and width (W_{FB}) under extreme wave conditions in offshore waters. This article provides a research basis for the experimental studies of fixed BDB and floating breakwater, presently under conduction at LABIMA the Laboratory of Maritime Engineering at the University of Florence (www.labima.unifi.it).

2 Materials and Methods

2.1 Numerical wave flume and fixed bottom-detached breakwater (BDB)

As shown in shown in Figure 1, a 20 m long NWF is divided into several regions, including air, water, refined and wave attenuating regions. The air and water regions are separated by free water surface. The height of NWF is 2 m while the water depth is 1.0 m. To capture the behaviour of free surface wave motion, the refined region is ± 0.1 m around the water surface (i.e. about \pm the maximum generated wave height). The wave attenuating region, a 3 m long numerical beach, is located at the end of NWF for absorbing incident waves thus avoiding the wave reflection caused by end of the NWF. Two Wave Gauges (WGs), WG-a and WG-b, are respectively installed 1.4 m and 7.0 m far from wave generation section.

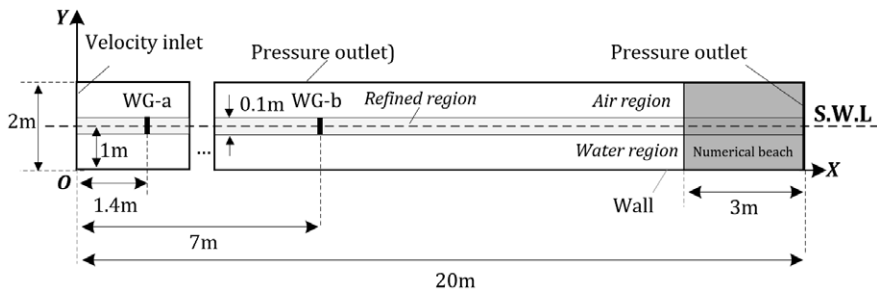


Figure 1 – Sketch of the 20 m long NWT.

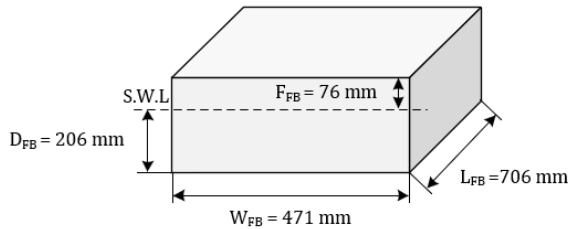


Figure 2 – Sketch of fixed BDB at a representative model scale 1:170.

In order to quantify the quality of wave generation in the NWF, the relative error (RE) and the wave decay coefficient (γ) as defined in Eq. 1 and Eq. 2 are used.

$$RE = \frac{H_0 - H_b}{H_0} \times 100\% \quad \text{Eq. 1}$$

$$\gamma = \frac{H_a - H_b}{H_a} \times 100\% \quad \text{Eq. 2}$$

where, H_a and H_b are the wave height measured by WG-a and WG-b, respectively; RE represents the relative error between the target wave height (H_0) and the practical wave height (H_b); γ is the decay of wave height between the wave height at the benchmark (H_a) and the practical wave height (H_b).

In offshore extreme weather, the designed BDB must provide a workable situation for the safe berthing of vessels. k_t is an important indicator, which is the ratio of transmitted wave height (H_t) over incident wave height (H_i) to evaluate the protection performance of BDB. Based on Macagno's formula [5,6] for selecting the necessary draft and width to limit k_t to acceptable values and considering the requirements for acceptable overtopping [11] for selecting the BDB's freeboard the designed dimensions of the BDB's model are shown in Figure 2 at the representative model scale (λ) 1:170.

2.2 Methods

ANSYS Fluent is a widely used CFD package, based on Finite Volume Method (FVM), to solve the complex phenomenon in wave-structure interaction, which can be described by continuity (Eq. 3) and N-S equations (Eq. 4) for incompressible and homogeneous fluids.

$$\frac{\partial u_i}{\partial x_i} = 0 \quad \text{Eq. 3}$$

$$\frac{\partial u_i}{\partial t} + u_j \frac{\partial u_i}{\partial x_j} = -\frac{1}{\rho} \frac{\partial p}{\partial x_i} + g_i + \frac{1}{\rho} \frac{\partial \tau_{ij}}{\partial x_j} \quad \text{Eq. 4}$$

where $i=1,2$ and $j=1,2$ for two-dimension flow; u_i : velocity components; p : pressure; g_i : gravitational acceleration components (just along the vertical axes); τ_{ij} : stress tensor. Those equations are based on time-averaging that introduces Reynolds stress terms associated with mean flow variables so that a turbulence closure model is needed. In this work, 2D numerical simulation is adopted.

Wave damping effects taking place during wave propagation along the NWF should be limited to realistic value. Based on the applicable range of wave theories, Stokes 2nd order wave was adopted to provide the reference for verifying the accuracy of wave generation [12]. The BDB is designed in offshore extreme weather for creating a safe zone with limited k_t up to extreme wave condition of 100-year return period. As reference value for the 100-year return period wave condition for the Mediterranean Sea, incident wave height (H_i) of 0.043 m, wave period (T_p) of 0.94 s, wavelength (L_w) of 1.39 m in a water depth (d_w) of 1.0 m, are selected for calibrating the NWF (the values are scale 1:170). Moreover, the influence of wave conditions and BDB design parameters were numerically studied even under the wider ranges comprising $H_i=0.01\sim 0.07$ m, $L_w=0.9\sim 3.1$ m, $D_{FB}=19\div 206$ mm and $W_{FB}=25\div 550$ mm.

In the NWF, the so-called Velocity Inlet is used for wave inlet boundary; Pressure Outlet is adopted for wave outlet and top boundaries; Wall type is adopted for seabed and BDB boundaries. The sub-models (Open Channel Wave BC and

Open Channel Flow [13]) in VOF are activated for generating wave at inlet boundary and attenuating wave in numerical beach. To cope with the spatial discretization, Least Square Cell Based was used for gradient. Modified Body Force Weighted was adopted for pressure. The air and water phases were incompressible and Modified High Resolution Interface Capturing method was used for defining the free surface. Spatial discretization is Second Order Upwind.

3 Results and Discussion

3.1 Calibration of NWF

The influence of different numerical settings (time step, turbulent model, velocity-pressure coupling method and transient formulation) on the accuracy of wave generation are studied. The free surface wave motions measured by WG-b by adopting various numerical settings are shown in Figure 3. In this work, the time step is 0.002 s; turbulent model is k-e RNG; Velocity-Pressure coupling method is PISO; Transient formulation is Second Order Implicit.

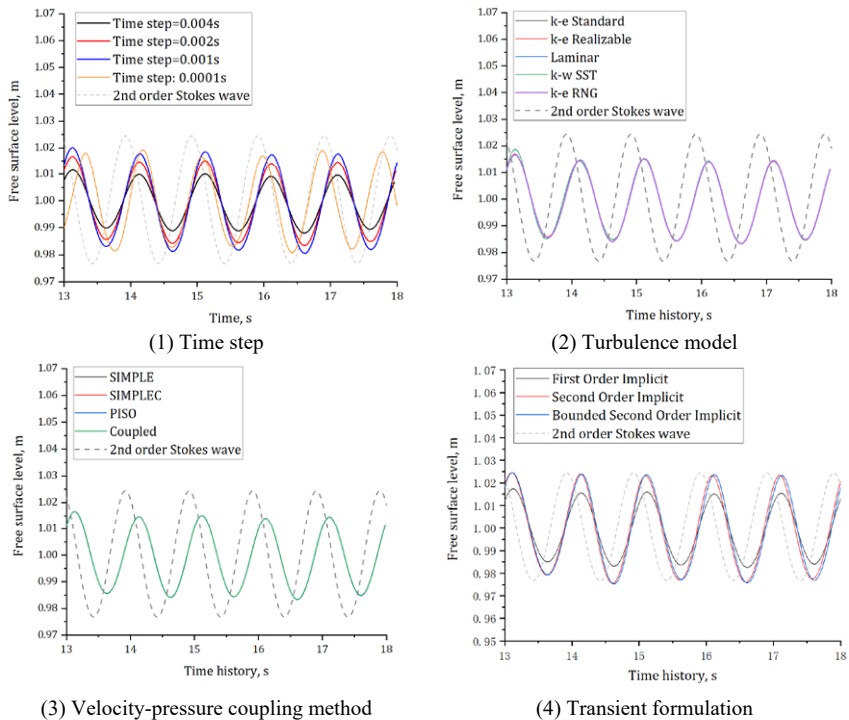


Figure 3 – The influence of different numerical settings on the free surface wave motion recorded by the WG-b (i.e, 7 m far from the wave generation section).

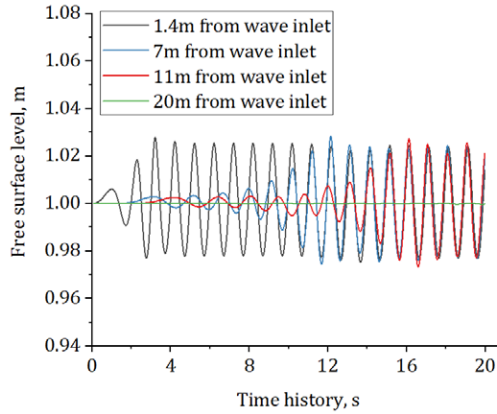


Figure 4 – Time histories of the free surface levels at different NWF sections (1.4 m, 7 m, 11 m and 20 m far from wave inlet).

Considering that when the transmitted wave reaches the end of NWF it is reflected by the wave outlet boundary, a Numerical Beach (wave attenuating region) was activated for attenuating the wave at the end of NWF thus limiting the reflection to tolerable values. The time histories of the free surface levels at different positions (1.4 m, 7 m, 11 m and 20 m far from wave inlet) along the 20 m NWF are shown in Figure 4. It shown that the free surface wave motion at the and of the NWF, i.e. 20 m far from the wave inlet, is much weaker compared with those measured in other positions, which indicates that the numerical beach efficiently attenuates wave energy. After 13 s, the free surface wave motion measured by WG-b becomes fully developed and stable.

Loose mesh scheme induces numerical inaccuracy and instability, and the over refined mesh scheme does not lead to better results and requires more time cost. To select the best compromise in term accuracy of results and computation efforts a sensitivity analysis on mash size was conducted, by using the 100-year return period wave condition, Figure 5. ρ_{ver} is the mesh resolution in the vertical direction in the refined region near the free surface; ρ_{hor} is the mesh resolution along the horizontal direction in NWF. Based on the wave height measured by WG-a and WG-b, the RE and γ that characterize the developed NWF can be controlled within 2 %, when $\rho_{hor}=80$ elements/ L_w and $\rho_{ver}=15$ elements/ H_i . When the BDB in installed into the NWT, the mesh resolutions near its the vertical and horizontal walls are 200 elements/ L_w and 62 elements/ H_i , respectively.

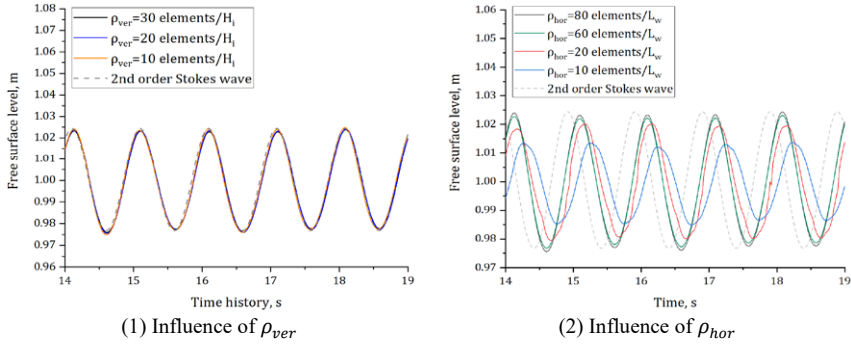


Figure 5 – Influence of the mesh resolutions on the free surface wave motion measured at WG-b located 7 m far from the wave inlet.

3.2 Verification of numerical tool

The experimental tests carried out by Liang et al. [3] were used for validating the reliability of the developed NWF in simulating the transmitted wave in the following test conditions: $W_{FB}=0.5$ m, $D_{FB}=0.16$ m, $W_{FB}/L_w=0.13-0.33$, $H_i=0.07$ m and $d_w=0.6$ m. The distance between the fixed BDB and wave inlet was 7 m, and the k_t was tested 0.33 m behind it. The comparison between the results of k_t from the numerical simulation of this work and the experimental result from Liang et al. is shown in Figure 6. The numerical results of k_t well match previous experimental results.

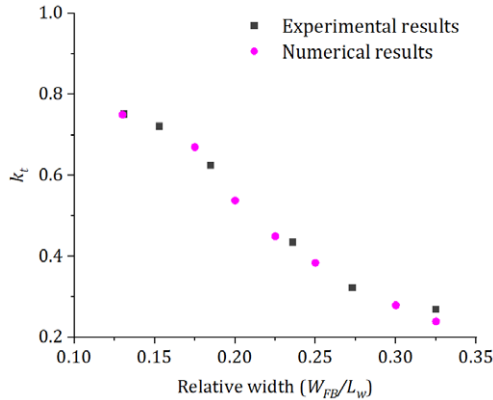
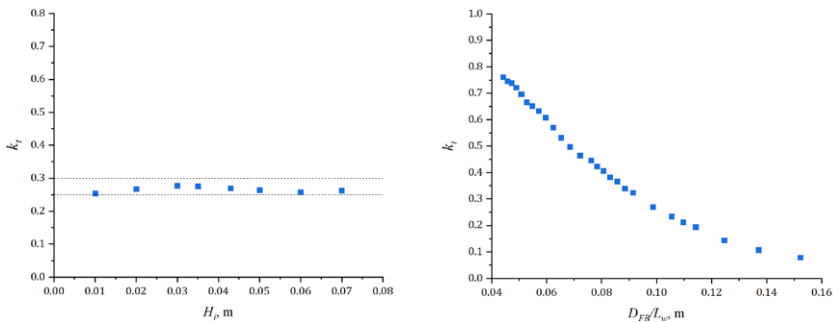


Figure 6 – Comparison between numerical results of k_t obtained via the NWT and experimental measurements from Liang et al. [3] ($W_{FB}=0.5$ m, $D_{FB}=0.16$ m, $W_{FB}/L_w=0.13\div 0.33$, $H_i=0.07$ m and $d_w=0.6$ m)

3.3 Sensitivity analysis of k_t to wave conditions and BDB's design parameters

The influence of H_i and L_w on the k_t of fixed BDB are shown in Figure 7. With the increasing of H_i , the change of k_t is small, but with the increasing of D_{FB}/L_w (here obtained by decreasing L_w), the k_t strongly decreases. Those are because the wave energy mostly concentrates near the free surface and for the fixed wave period used in the tests with varying H_i it is almost blocked by BDB thus the change of H_i has little influence on k_t . On the contrary, with the decreasing of D_{FB}/L_w by increasing the wave period and so by increasing the wavelength more wave energy is driven by wave and passes beneath the BDB, which causes the increment of k_t [12].

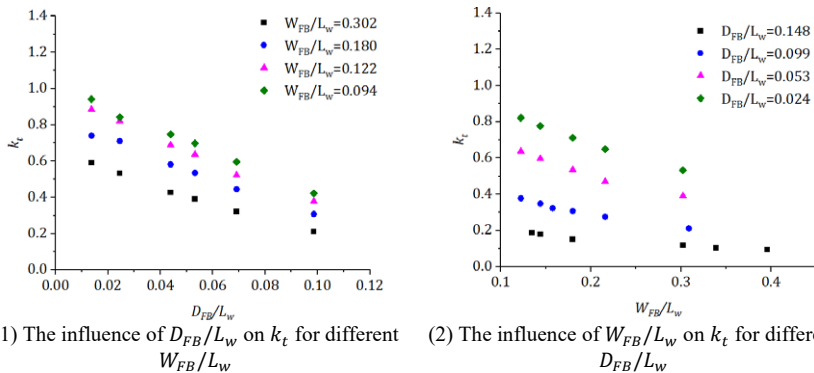
Due to the extreme weather in offshore environment, the dimensions of BDB are very large, which leads to expensive investment cost of materials, and should be optimized for avoiding over engineering design. The influence of relative width (W_{FB}/L_w) and relative draft (D_{FB}/L_w) on the k_t of BDB under the selected 100-year return period wave condition are shown in Figure 8. With the increment of D_{FB}/L_w and W_{FB}/L_w the k_t decreases because larger D_{FB} values block a larger part of the wave energy and because larger W_{FB} values induce larger hydrodynamic damping.



(1) The influence of H_i on k_t .

(2) The influence of D_{FB}/L_w on k_t .

Figure 7 – The influence of H_i and L_w on the k_t of deep-draft fixed BDB ($H_i=0.01\sim 0.07$ m, $L_w=0.9\sim 3.1$ m, $D_{FB}=206$ mm and $W_{FB}=471$ mm).



(1) The influence of D_{FB}/L_w on k_t for different W_{FB}/L_w

(2) The influence of W_{FB}/L_w on k_t for different D_{FB}/L_w

Figure 8 – The influence of the BDB's design parameters on k_t under the 100-year return period wave condition ($H_i=0.043$ m, $T_p=1.0$ s, $D_{FB}=19\div 206$ mm and $W_{FB}=25\div 550$ mm).

4 Conclusion

A reliable NEW for studying the interaction between extreme waves and deep-draft fixed BDB was developed. The reliability of the developed NWF for measuring the k_t of BDB was verified throughout comparison with available experimental measurements conducted by other authors. The influence of wave conditions on the k_t of deep-draft fixed BDB was examined. The results indicate that H_i has a minimal impact on k_t , while D_{FB}/L_w significantly affects k_t . As D_{FB}/L_w decreases (L_w increases), k_t increases, as longer waves drive more energy propagating beneath the BDB bottom. As W_{FB}/L_w increases the k_t decreases because increased hydrodynamic damping caused by the larger W_{FB} .

This work serves as the seed study for the further development of the work on floating structures and mooring system.

Acknowledgements

This work is supported by the Tuscany Region (TR) administration, under the PEGASO initiative, that financed the PhD scholarship of Zihan Liu, and by AM3 Spinoff s.r.l. the spinoff company of the Florence University (AM3-UNIFI) that is co-financing Zihan Liu with an internship and it is partner of the Joint Laboratory A-MARE, www.amare.unifi.it. TR and AM3-UNIFI are gratefully acknowledged.

Reference

- [1] Bouchet R, Troya L, Sedillot F, Peset L, Jaeger JM, Martareche F (2004) - *Monaco semi-floating dyke a 352 metre long concrete caisson*. Proc Fib Symp 2004 - Concr Struct Chall Creat 2004:109–26.
- [2] Koutandos E., Prinos P., Gironella X. (2005) - *Floating breakwaters under regular and irregular wave forcing: reflection and transmission characteristics*. Journal of Hydraulic Research, 43(2), 174–188.
- [3] Liang J ming, Liu Y, Chen Y kun, Li A jun (2022) - *Experimental study on hydrodynamic characteristics of the box-type floating breakwater with different mooring configurations*. Ocean Eng (254), 111296.
- [4] Wu JP, Mei TL, Zou ZJ (2022) - *Experimental study on wave attenuation performance of a new type of free surface breakwater*. Ocean Eng (244), 110447.
- [5] Ruol P, Martinelli L, Pezzutto P (2013) - *Formula to Predict Transmission for π -Type Floating Breakwaters*. Volume 139 (1).
- [6] Kolahdoozan M, Bali M, Rezaee M, Moeini MH (2017) - *Wave-Transmission Prediction of π -Type Floating Breakwaters in Intermediate Waters*. J Coast Res (33), 1460–1466.
- [7] Ruol P, Martinelli L, Pezzutto P (2012) - *Limits of the new transmission formula for n -type floating breakwaters*. Proc Coast Eng Conf 2012:1–10.
- [8] Ursell F (1947) - *The effect of a fixed vertical barrier on surface waves in deep water*. Math Proc Cambridge Philos Soc (43), 374–82.
- [9] Vinet L, Zhedanov A (2011) - *A “missing” family of classical orthogonal polynomials*. J Phys A Math Theor (44), 1689–99.
- [10] Paotonan C, Umar H, Rahman S, Rahman T (2022) - *Analytical Approach of Wave Transmission Coefficient through on Composite Hanging Breakwater*. IOP Conf Ser Earth Environ Sci.

- [11] Agency EAE, Enw UK, Netwerk E, Kuratorium NLK (2007) - *Wave overtopping of sea defences and related structures: Assessment manual*. Kuste, 1–171.
- [12] Holthuijsen LH (2007) - *Waves in oceanic and coastal waters*. Waves Ocean Coast Waters (9780521860), 1–387.
- [13] Xu G, Niu G, Lu T, Li H, Wang S (2020) - *Water wave decay and run-up in the numerical water wave tank*. Desalin Water Treat (188), 375–389.